https://doi.org/10.1016/j.polymer.2021.123961

Photo- and pH-responsive drug delivery nanocomposite based on o-nitrobenzyl functionalized upconversion nanoparticles

Xiaotao Wang[a*], Chuang Liu[a], Yebing Yang[a], Huiling Guo[a], Zhuofan Chen[a], Junyong Xia[a], Yonggui Liao[b,*], Chak-Yin Tang [c], Wing-Cheung Law[c,*]

[a]*Hubei Provincial Key Laboratory of Green Materials for Light Industry, Collaborative Innovation Center for Green Light-weight Materials and Processing, School of Materials Science and Engineering, Hubei University of Technology, Wuhan, 430068, China*

[b]*Key Laboratory for Material Chemistry for Energy Conversion and Storage, Ministry of Education, Hubei Engineering Research Center for Biomaterials and Medical Protective Materials, Hubei Key Laboratory of Material Chemistry and Service Failure, School of Chemistry and Chemical Engineering, Huazhong University of Science and Technology, Wuhan 430074, China*

[c]*Department of Industrial and Systems Engineering, The Hong Kong Polytechnic University, Hung Hom, Kowloon, Hong Kong, China*

[*] Corresponding Authors: xiaotaowang@hbut.edu.cn (X. Wang), ygliao@mail.hust.edu.cn (Y. Liao), roy.law@polyu.edu.hk (W. Law)

Abstract: A near infrared (NIR) and pH dual-responsive nanocomposite, composed of a lanthanide-doped upconversion nanoparticle (UCNP) core and a transformable poly-o-nitrobenzyl shell, is prepared by distillation precipitation polymerization and template method. The poly-o-nitrobenzyl shell can undergo hydrophobic-hydrophilic transformation upon an irradiation of 980 nm, rendering the capability of NIR-activated drug release. Anticancer drug, doxorubicin (DOX), can be loaded into these nanocomposites with a loading efficiency of 7.23 wt%. Furthermore, a pH responsiveness caused by the hydrogen bond and charge interactions between DOX and nanocapsules can be triggered the release of drugs at low pH. Under visible light irradiation and neutral (pH 7.4) conditions, the cumulative release of DOX is only 8.35% after 300 min, while it reaches 59.5% under a synergistic effect of NIR irradiation and acidic conditions. Baker-Lonsdale model has been used to describe the drug release kinetics of this system, and the diffusion coefficient ($3DC_s/r_0^2C_0$) and R^2 under different conditions are determined to be 4.15×10^{-6} and 0.98 (pH 7.4 and visible light), 2.64×10^{-5} and 0.99 (NIR light), 3.26×10^{-5} and 0.97 (pH 4.5 and visible light), 2.59×10^{-4} and 0.99 (pH 4.5 and NIR light), respectively. This controlled release feature makes the nanocomposite a promising therapeutic agent for treating diseases.

1. Introduction

In recent years, there is an increasing interest in designing responsive drug carriers, in which the controlled release of loaded drugs under specific conditions can effectively improve the efficacy of existing drugs and reduce the side effects of drugs [1-5]. This requires the drug carrier to be responsive to external stimuli (temperature, pH, light, ultrasound, electric/magnetic field, etc.) [6-10]. Due to the complicated environments of human beings, the use of external stimulation for controlled drug release is of great advantages. Among different exogenous stimuli, light irradiation is favorable because of its advantages of flexibility, controllability and less invasive [11, 12].

The photoresponsive behavior is always conferred by block polymer (BCP) micelles including polyazobenzene, spiropyran, coumarin, or o-nitrobenzyl [13-17]. The photoisomerization is triggered by an irradiation of UV light. The photoresponsive behavior of micelle could include: (i) shifting of hydrophobic-hydrophilic balance, (ii) breaking of block junction, (iii) degradation of main chain, and (iv) reversible cross-linking [18]. Zhao et al [19] synthesized a UV responsive micelle constructed of amphiphilic block copolymer PAzoMA-b-PAA, in which azobenzene groups were acted as the hydrophobic segment side chain. After UV irradiation, polarity of azobenzene changed and the hydrophilic equilibrium was destroyed, thus releasing the drug payload. A new type of carrier for loading cholesterol was designed by grafting coumarin on mesoporous silicon nanoparticles [20]. O-nitrobenzyl (O-NB) compound was a kind of photoresponsive element that attracted broad interest due to its variety, relatively simple synthesis method and rapid photo cracking process. The light energy induces the rearrangement of charges and recombination of chemical bond in the o-nitrobenzyl compound, producing the photolysis product o-nitro-aromatic aldehyde/ketone and small molecules. Dong et al [21]

synthesized photoresponsive polymer poly(S-(o-nitrobenzyl)-L-cysteine)-b-poly(ethylene glycol) (PNBC-b-PEO), which could form stable spherical micelles with a particle size of about 79 nm in water. When these micelles were exposed in UV light, the particle size would decrease and the micelles would eventually rupture in a prolonged irradiation.

Most of photoresponsive polymers absorb UV light to activate a specific photochemical reaction. However, UV light is toxic to living cells, and the depth of penetrating tissue is poor [22, 23]. NIR light is preferable to act as a stimulus light source in the field of biomedicine. Upconversion nanoparticles (UCNPs) can absorb NIR light and emit UV and visible lights, which is a promising agent to link the photoresponsive polymers with near infrared (NIR) light [24, 25]. Zhao et al [26] encapsulated UCNPs inside micelles of poly(ethylene oxide)-block-poly(4,5-dimethoxy-2-nitrobenzyl methacrylate). The photo cleavage reaction could be activated under NIR light that led to the dissociation of BCP micelles. The NIR light-responsive nanovector could be prepared through electrostatic interaction-driven complexation between the negatively charged silica-coated UCNPs and positively charged UV-labile polyelectrolyte bearing pendant poly(ethylene glycol) and o-nitrobenzyl side groups, which could result in the release of molecules through the cleavage of o-nitrobenzyl to disrupt the balance of electrostatic self-assembled structure [27]. Almutairi et al [28] reported an upconversion of NIR light for efficient polymeric nanoparticle degradation and cargo release through electrospray in which two or more UCNPs could be encapsulated inside the polymeric matrix to form nanocomposite materials. Nonetheless, the development of drug loaded UCNPs-polymer nanocarriers with stable structures and NIR controlled release properties remains a hot research area.

In this work, a core-shell structured nanocapsules that is composed of an inorganic UCNPs as the core and a transformable poly(4,5-dimethoxy-2-nitrobenzyl methacrylate) (PNBMA) shell

layer. The fabrication and drug loading processes are shown in Scheme 1. The UCNPs could convert NIR light to UV which can be absorbed by PNBMA shell, resulting in the photolysis of PNBMA that alters the hydrophilicity. Silica coated UCNPs (UCNPs@SiO_2) was used as the synthesis templates. 4,5-Dimethoxy-2-nitrobenzyl methacrylate monomers were crosslinked by ethylene glycol dimethacrylate (EGDMA) at the surface of UCNPs@SiO_2, yielding the UCNPs@SiO_2@PNBMA/MAA nanoparticles by distillation precipitation polymerization. Anticancer drug, doxorubicin (DOX), was then loaded into the HF-etched UCNPs@PNBMA/MAA nanocapsules for controlled release behavior.

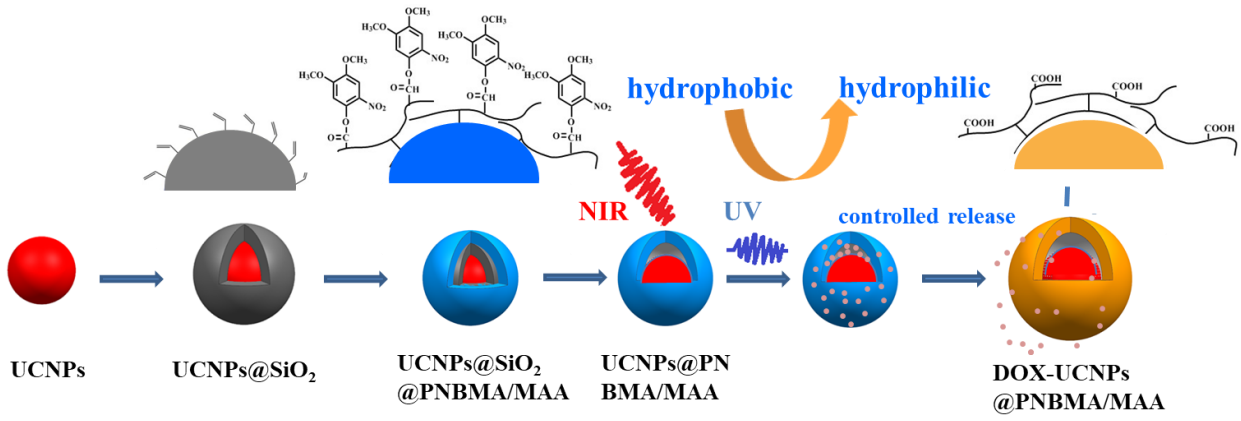

Scheme 1. The fabrication of UCNP@SiO_2@PNBMA/MAA nanocapsules and the DOX loading and release.

2. Experimental Section

2.1. Materials

Rare earth oxides (Y_2O_3, 99.99%; Yb_2O_3, 99.99%; Tm_2O_3, 99.95%) were obtained from Yuelong New Material Co., Ltd. Oleic acid (OA, 90%), 1-octadecene (ODE, 95%), 4,5-dimethoxy-2-nitrobenzyl alcohol (98.0%), hydroquinone, 3-(hydroxymethyl)-4-nitrophenol (98%), N,N′-dicyclohexylcarbodiimide (DCC, 99.0%), 4-dimethylaminopyridine (DMAP, 99%),

3-(trimethoxysilyl) propyl methacrylate (97%) and ethylene glycol dimethacrylate (EGDMA, 98%) were purchased from Aladdin Reagent Co., Ltd. Sodium hydroxide, ammonium fluoride, hydrochloric acid (HCl, 36.7%), ethanol, chloroform, cyclohexane, ammonia aqueous solution (33 wt%), tetraethyl orthosilicate (TEOS), methacrylic acid were supplied by Sinopharm Group Chemical Reagent Co., Ltd. Igepal CO-520 was purchased from Sigma-Aldrich Trading Co., Ltd.

2.2. Synthesis of $NaYF_4$: Yb^{3+}/Tm^{3+} nanoparticles ($NaYF_4$: Yb/Tm)

The $NaYF_4$: Yb^{3+}/Tm^{3+}nanoparticles were synthesized using solvothermal procedure based on the previously reported method [29]. Typically, 0.2 mol/L YCl_3 aqueous solution, 0.2 mol/L $YbCl_3$ aqueous solution, 0.1 mol/L $TmCl_3$ aqueous solution, 0.5 mol/L NaOH methanol solution and 0.5 mol/L NH_4F methanol solution were prepared for use. YCl_3 (3.975 mL, 0.975 mmol), $YbCl_3$ (1 mL, 0.2 mmol), $TmCl_3$ (50 μL, 5 μmol) were mixed in a 100 mL four-necked round-bottom flask and were heated to remove moisture, 7 mL of oleic acid and 15 mL of 1-octadecene were added into the reaction flask, nitrogen gas was introduced into the flask. The mixture was heated to 120 ℃ to get rid of water and oxygen. After about 10 min, it was heated to 160 ℃ and held for 40 min to get a yellow transparent solution. Turning off the heating and slowly cool the solution to room temperature, a mixed solution of NaOH-methanol stock solution (5 mL) and NH_4F-methanol stock solution (8 mL) was added to the reaction flask, stirring at room temperature for 1 h. The mixture was slowly heated to 50 ℃ and maintained for 30 min to complete nucleation. Then, the solution was heated to 120 ℃ under a nitrogen flow to remove methanol. When the solution become clear, the mixture was quickly heated to 300 ℃ and kept for 1.5 h. After cooling down to room temperature, the nanoparticles ($NaYF_4$: Yb^{3+}/Tm^{3+}) were obtained by centrifugation (8000 rpm, 40 min) and washed with a mixture of ethanol and

chloroform (6/1, v/v) for three times. Finally, the purified $NaYF_4$: Yb^{3+}/Tm^{3+} were dispersed and stored in chloroform.

2.3. Synthesis of OA-NaYF4: $NaYF_4$: Yb^{3+}/Tm^{3+}core-shell nanoparticles (UCNPs)

The UCNPs were made by coating $NaYF_4$: Yb^{3+}/Tm^{3+} with a homogeneous shell using the same method as described above. Typically, YCl_3 (5 mL, 1 mmol) was added in a 100 mL four-necked round-bottom flask and were heated to remove moisture, 7 mL of oleic acid and 15 mL of 1-octadecene were added into the reaction flask, nitrogen gas was introduced into the flask and the nitrogen atmosphere was maintained. The mixture was heated to 120 °C to get rid of water and oxygen. After about 10 min, heating to 160 °C and hold for 40 min to get a yellow transparent solution. Stopped heating and until the mixture cooled down to room temperature, taking about 9 mL of the chloroform solution with $NaYF_4$: Yb/Tm prepared and added it into the reaction flask. Then, the mixture was heated to 90 °C under nitrogen flow and maintained at this temperature for a while to remove chloroform. Stopped heating and cooled the mixture to room temperature again, a mixed solution of NaOH-methanol stock solution (5 mL) and NH_4F-methanol stock solution (8 mL) was added to the reaction flask, stirred at room temperature for 1 h. The mixture was slowly heated to 50 °C and maintained for 30 min to complete nucleation. Then, the solution was heated to 120 °C under a nitrogen flow to remove methanol. When the solution became clear, the mixture was quickly heated to 300 °C and kept for 1.5 h. After the reaction was cooled, the UCNPs were obtained by centrifugation (8000 rpm, 40 min) and washed with a mixture of ethanol and chloroform (6/1, v/v) for three times. Finally, the purified UCNPs nanoparticles were dispersed and stored in cyclohexane.

2.4. Coating of silica on the UCNPs (UCNPs@SiO_2)

Silica was coated on the surface of the prepared UCNPs particles by reverse microemulsion method for surface modification. Briefly, IGEPAL CO-520 (1.3 mL), cyclohexane (20 mL) and cyclohexane solution with the UNCPs (0.7 mL) were mixed in 100 mL flask under magnetic stirring for 10 min. Then, ammonia aqueous solution (160 μL) was added into the flask and took the mixture in ultrasound bath for 30 min to form a transparent microemulsion. Next, TEOS (250 μL) was added to synthesize a shell of silica. Subsequently, methacryl-oxypropyltrimethoxysliane (2.5 mL) was added to the mixture under stirring for 24 h to functionalize the particles surface. The product (UCNPs@SiO_2) were obtained by centrifugation (1200 rpm, 45 min) and washed with a mixture of ethanol and acetone (6:1, v/v) three times. Finally, the purified UCNPs nanoparticles were dispersed and stored in ethanol.

2.5. Synthesis of the monomer 4,5-dimethoxy-2-nitrobenzyl methacrylate (NBMA).

In a 100 mL flask, 5-dimethoxyl-2-nitrobenzyl alcohol (1.49 g) was dissolved in dichloromethane (25 mL), which was then placed in an ice bath. DCC (5 g) was dissolved in dichloromethane (15 mL) and the mixed solution was slowly added to the flask. Then, 0.7 mL of methacrylic acid, 0.025 g of DMAP and 15 mL of dichloromethane were slowly added to the flask, and stirred at room temperature for 2 d. Insoluble impurities that are removed in solvent by filtration, the obtained filtrate was first washed with 15% $NaCO_3$ solution 3 times, and then washed with saturated NaCl solution until neutral, and finally drying by magnesium sulfate. After filtration, the filtrates was concentrated into solid and dried under vacuum overnight.

2.6. Synthesis of UCNPs@SiO_2@PNBAM/MAA

Photoresponsive PNBMA/MAA shell was coated on UCNPs@SiO_2 surface by distillation precipitation polymerization. Typically, in a 100 mL flask, 10 mg of vacuum-dried

UCNPs@SiO_2 nanoparticles were dispersed in 72 mL of acetonitrile and stirred for 30 min. Then, adding NBMA (0.24 g), EGDMA (90 μL), MAA (75 mL) and AIBN (2.87 mg) into the flask in turn, which was then placed in an oil bath, equipped with an oil-water separator, a condenser, a receiver and nitrogen protection device. Under the protection of nitrogen atmosphere, the reaction mixture was heated from room temperature to 80 °C within 30 min and kept for 15 min, then heated to 100 °C, maintained at this temperature for 3 h and distilled 36 mL acetonitrile. Turned off the heating and added a small amount of hydroquinone inhibitor to stop the reaction. After the resultant mixture was cooled down to room temperature, UCNPs@SiO_2@PNBMA/MAA were obtained by centrifuging the obtained solution (1400 rpm, 45 min) and washed with ethanol about three times. Finally, the product was dispersed in ethanol solution for storage.

2.7. Synthesis of UCNPs@PNBAM/MAA nanocapsules

UCNPs@PNBMA/MAA nanocapsules were prepared by etching the silica layer of UCNPs@SiO_2@PNBMA/MAA nanoparticles. The above nanoparticles were dispersed in 3 mL of ethanol solution, and then 2 mL HF was add to it and stirred for 48 h. The resultant products were purified by about three cycles of centrifugation.

2.8. Light responsive behavior of UCNPs@PNBAM/MAA nanocapsules

UCNPs@PNBMA/MAA (10 mg) nanocapsules were dispersed in 20 mL of water, then poured it into the dialysis tubes (molecular weight cutoff of 8000-14000), and sealed both ends. The dialysis tubes were placed in a beaker containing 20 mL of deionized water and submerged the dialysis tubes with deionized water. Under NIR irradiation, the solution was taken out from the beaker for UV measurement at intervals.

2.9. Loading of doxorubicin (DOX)

30 mg UCNPs@PNBMA/MAA nanocapsules were dispersed in 18 mL DOX aqueous solution (2 mg/mL) and stirred with magnetic force under normal temperature and dark conditions for 24 h. DOX-UCNPs@PNBMA/MAA nanocapsules were obtained by centrifuging the obtained solution (1400 rpm) and washed with ethanol about three times to remove unsupported DOX molecules. The DOX solution before and after loading was diluted 10 times, and the absorbance of both at 480 nm was measured by UV-vis absorption spectroscopy to calculate the drug loading capacity.

2.10. pH-triggered release behavior of DOX-UCNPs@PNBMA/MAA

Taking 8 mg of DOX-UCNPs@PNBMA/MAA nanocapsules and disperse them in 1 mL of aqueous solutions at pH 4.5, then package the mixture into a dialysis bag with a molecular weight cut-off of 8000-14000. The dialysis bag was immersed in 5 mL of pH 4.5 aqueous solutions. The solution outside the dialysis bag was taken at regular intervals to measure the absorption peak intensity at 480 nm with an ultraviolet spectrophotometer to calculate the release amount. The experimental method of release behavior under the condition of pH 7.4 is the same, except that the liquid is replaced with neutral deionized water.

2.11. Photo-triggered release behavior of DOX-UCNPs@PNBMA/MAA nanocapsules

8 mg of DOX-UCNPs@PNBMA/MAA nanocapsules were dispersed in 1 mL of aqueous solution at pH 4.5. Then, the mixture was packaged into a dialysis bag with a molecular weight cut-off of 8000-14000. The dialysis bag was immersed in 5 mL of pH 4.5 aqueous solution with NIR light irradiation. The solution outside the dialysis bag was taken at regular intervals to measure the absorption peak intensity at 480 nm with an ultraviolet spectrophotometer to

calculate the release amount.

3. Results and Discussion

3.1. Morphology of UCNPs@PNBMA/MAA nanocapsules

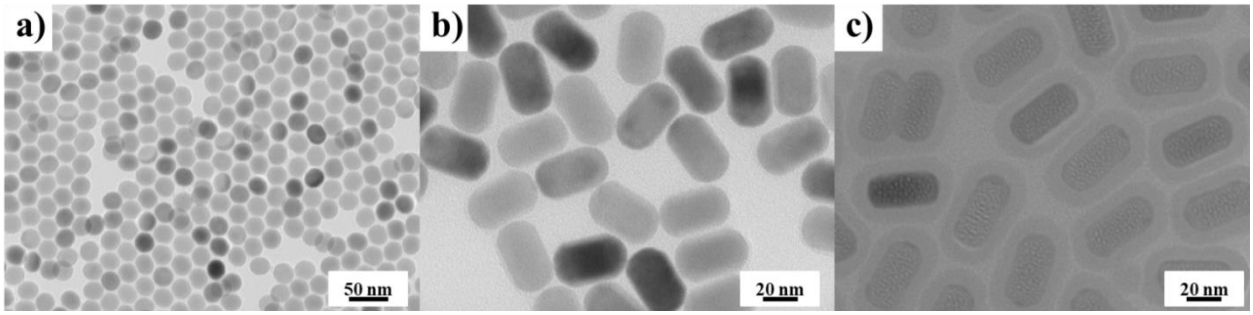

Fig. 1. TEM images of (a) $NaYF_4$: Yb^{3+}/Tm^{3+}, (b) UCNPs, (c) UCNPs@SiO_2nanoparticles.

The morphological structures of the prepared $NaYF_4$: Yb^{3+}/Tm^{3+}, UCNPs and UCNPs@SiO_2 particles were investigated by TEM. As shown in Fig. 1a, the $NaYF_4$: Yb^{3+}/Tm^{3+} particles are spherical and the average diameter is about 25 nm. A homogeneous $NaYF_4$ shell was coated on the $NaYF_4$: Yb^{3+}/Tm^{3+} particles surface to improve its surface defects [30] and the luminescence effect. If the concentration of oleic acid ligand is different, the growth rate of different crystal planes of β crystalline $NaYF_4$: Yb^{3+}/Tm^{3+}nanoparticles are also different. The increase of oleic acid content leads to the dominant growth rate of the particle in the [0001] crystal plane, and the particle finally presents an ellipsoid with a size of 42 nm × 25 nm (Fig. 1b). The surface of UCNPs particles was then coated with a layer of silica by reverse microemulsion method to improve the hydrophilicity of the UCNPs particles [31, 32]. In Fig. 1c, a clear UCNPs@SiO_2 double-layer structure can be observed, and the thickness of the silica layer is about 12 nm. The FT-IR spectra of OA–UCNPs, UCNPs@SiO_2, UCNPs@SiO_2@PNBMA/MMA particles were further proved the different structure in Fig. S1.

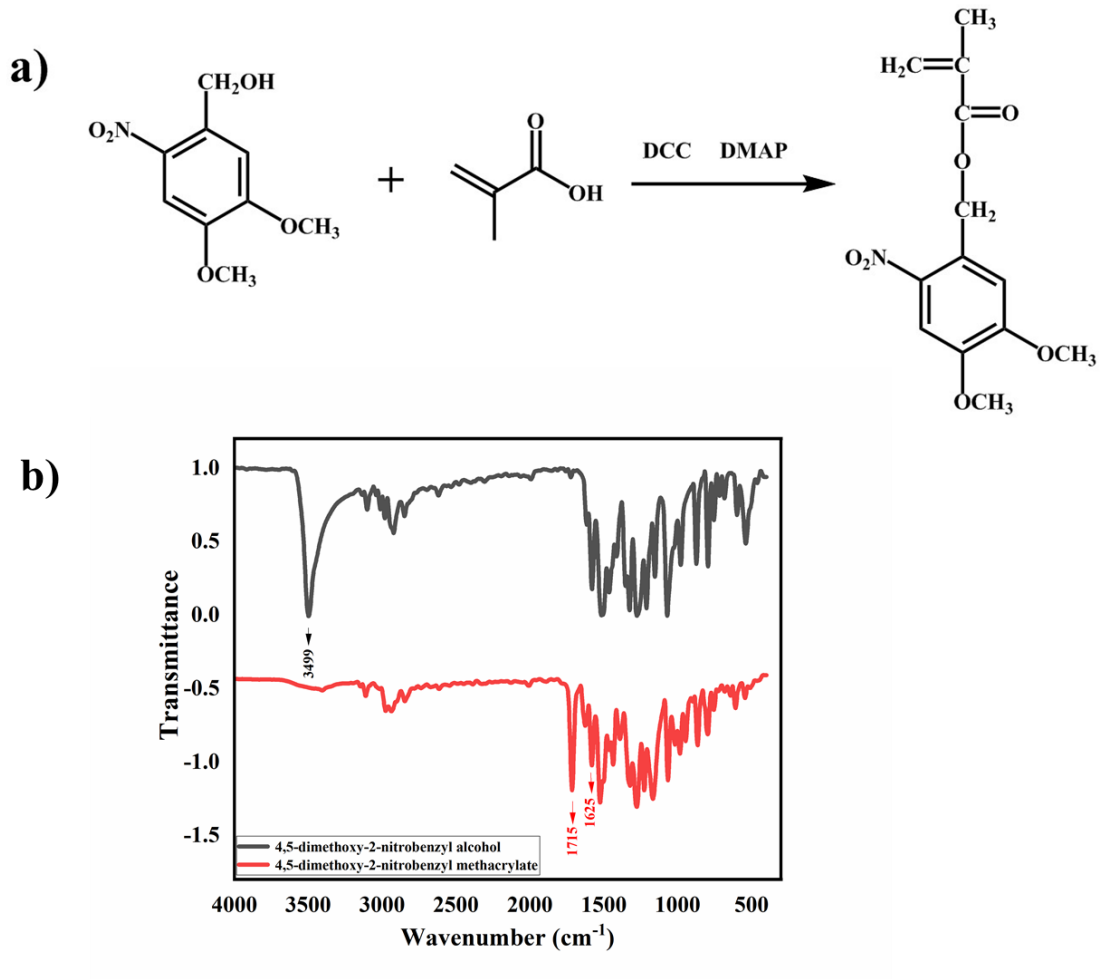

Fig. 2. Synthesis routes of (a) the photoresponsive monomer 4,5-dimethoxy-2-nitrobenzyl methacrylate (NBMA) (b) Fourier transform infrared (FT-IR) spectra of NBMA and 4,5-dimethoxy-2-nitrobenzyl alcohol.

The photoresponsive monomer 4,5-dimethoxy-2-nitrobenzyl methacrylate (NBMA) was synthesized from 4,5-dimethoxy-2-nitrobenzyl alcohol and methacrylate (Fig. 2a). Fig. 2b shows the Fourier transform infrared (FT-IR) spectra of NBMA. It can be observed that the symmetrical stretching vibration and asymmetric stretching vibration of nitro on benzene ring corresponds to two absorption peaks at 1322 cm^{-1} and 1525 cm^{-1}. The symmetrical stretching vibration and asymmetric stretching vibration of methoxy on benzene ring corresponds to two

absorption peaks at 1018 cm^{-1} and 1276 cm^{-1}. The stretching vibration of C=C can be attributed to the characteristic absorption peak at 1625 cm^{-1}. The stretching vibration of carbonyl corresponds to the characteristic absorption peak at 1715 cm^{-1}. By comparing the chemical formula as of 4,5-dimethoxy-2-nitrobenzyl alcohol and 4,5-dimethoxy-2-nitrobenzyl methacrylate, the absorption peak of hydroxyl group disappeared, and the absorption peak of C=O and C=C appeared, which was the evidence to the formation of NBMA.

UCNPs@SiO_2@PNBAM/MAA nanoparticles were synthesized through novel distillation precipitation polymerization method (Scheme 1). Typically, UNCPs@SiO_2 was used as template, MAA and NBMA were used as monomers, EGDMA was used as cross-linker, and acetonitrile was used as solvent. The shell thickness and dispersibility of UNCPs@SiO_2@PNBMA/MAA nanoparticles have been systematically investigated through the amount variation of monomer, cross-linker and solvent.

The thickness of UCNPs@SiO_2@PNBMA/MAA nanoparticles were regulated by changing the amount of monomer NBMA and MAA. In fact, increasing the amount of solvent is good for the dispersity of UCNPs@SiO_2@PNBMA/MAA nanoparticles but decreasing the monomer conversion. Distillation precipitation polymerization has the advantage that lower monomer concentration is used at the beginning of the reaction to ensure the dispersion of particles. When the reaction was carrying on, the solvent distilled constantly out of the system to increase the monomer conversion. For the large steric hindrance of photoresposive monomer, the distillation precipitation polymerization is a good method to synthesize disperse and robust photoresponsive nanoparticles [29]. When 0.176 g NBMA and 23.9 μL MAA were involved in the reaction (Fig. 3a), there was only about 2 nm thick layer of PNBMA/MAA on the surface of the UCNPs@SiO_2 nanoparticles. With increasing the amount of NBMA and MAA to 0.198 g and 60 μL

respectively, the thickness of the PNBMA/MAA shell increased to approximately 5 nm (Fig. 3b). When the amounts of NBMA and MAA were further increased to 0.247 g and 75 μL, the clear UCNPs@SiO_2@PNBMA/MAA three-layer structure was obtained with thickness about 7 nm (Fig. 3c). Crosslinking agent content and the amount of solvent acetonitrile were both used to optimize the morphological of UCNPs@SiO_2@PNBMA/MAA nanocomposites (Figs. S2 and S3, respectively). UCNPs@PNBMA/MAA nanocapsules were obtained by etching SiO_2 layer with HF (Fig. 3d).

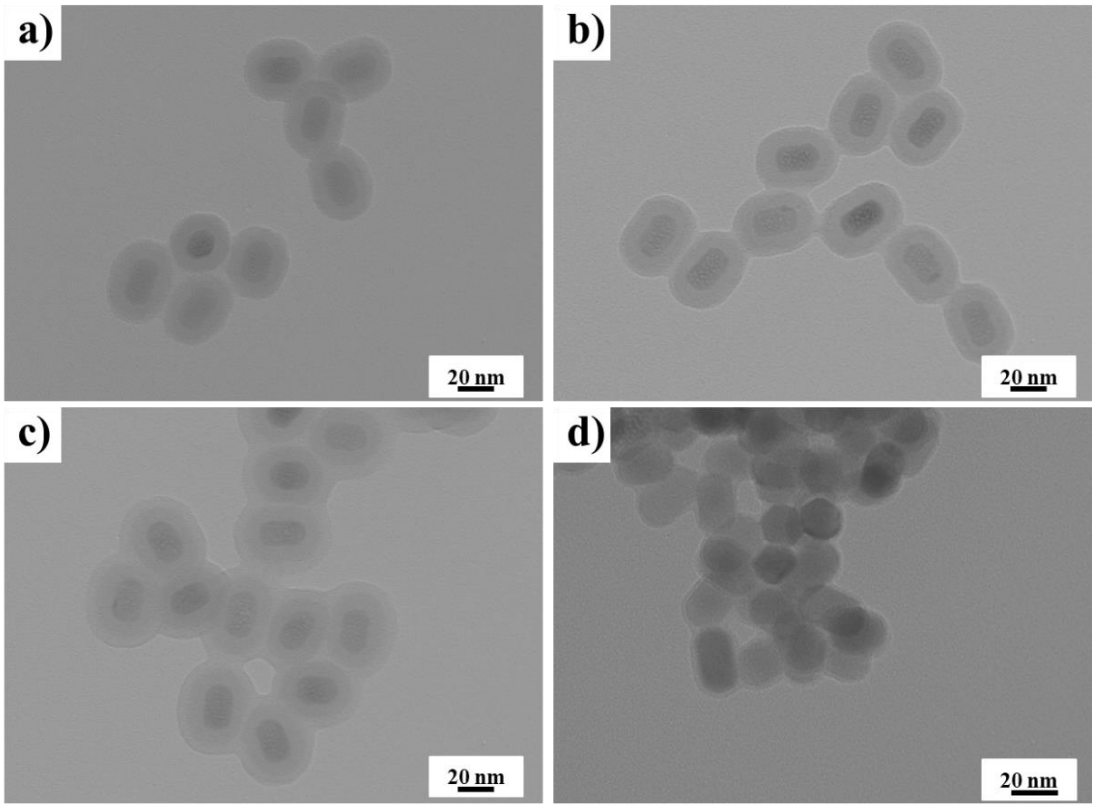

Fig. 3. TEM images of particles prepared under different amount of NBMA and MAA: (a) 0.176 g, 23.9 μL; (b) 0.198 g, 60 μL; (c) 0.247 g, 75 μL; (d) TEM image of UCNPs@PNBMA/MAA nanocapsules.

3.2. NIR light responsive properties of UCNPs@PNBMA/MAA nanocapsules

Fig. 4a shows the luminescent spectra of UCNP and UCNP@PNBMA/MAA nanocapsules disperse in ethanol under 980 nm NIR light irradiation. The emission bands of the UCNP luminescence spectrum include ~ 365 nm ($^1D_2$-$^3H_6$), ~ 450 nm ($^1D_2$-$^3H_4$) and ~ 475 nm ($^1G_4$-$^3H_6$). The band diagram is showed in Fig. S4. The solution of UNCPs emitted UV light under the absorption of NIR irradiation. UCNPs@PNBMA/MAA nanocapsules have no luminescence at 365 nm as compared with UCNPs, which could be deduced that the UV light emitted by the UCNPs is absorbed by O-NB. Furthermore, the solution of UCNPs@PNBMA/MAA nanocapsules changed to blue color compared to the violet emitted by pure UCNP upon 980 nm NIR light.

As shown in Fig. 4b, PNBMA undergoes photo-cleavage reaction upon 365 nm UV light irradiation. After absorbing 365 nm photons, a series of intermolecular charge rearrangement occur, resulting in the breaking of ester group to form carboxylic acids and o-nitrobenzaldehyde. The UCNPs@PNBMA/MAA nanocapsules were dissolved in deionized water to make solution with a concentration of 0.5 mg/mL. As shown in Fig. 4c, in the absence of NIR irradiation, the UV-Vis spectrum of the solution that outside the dialysis tubes did not change even after 24 h. However, under the NIR irradiation, the absorption bands, corresponding to photochromic o-nitrosobenzaldehyde, were detected in 350 ~ 450 nm regions. With the irradiation time increasing, the characteristic absorption peak at about 350 nm, originated from the o-nitrobenzaldehyde generated by the photo-cleavage reaction, gradually increased. With ester group transforming to carboxylic acids, the UCNPs@PNBMA/MAA nanocapsules would be more hydrophilic after the photo-cleavage reaction.

The dynamic light scattering (DLS) results (Fig. 4d) further reveals that the size of UCNPs@PNBMA/MAA nanocapsules increases from initial 108 nm to 140 nm after 20 min of

NIR irradiation. The change of hydrodynamic diameter was caused by the photo-cleavage reaction of o-nitrobenzyl ester, in which the hydrophobic ester group was transformed to hydrophilic carboxylic acid. Zhao also demonstrate that the photoresponsive micelles constructed of poly(nitrobenzyl methacrylate) block polymer would be activated the photo-cleavage reaction upon 980 nm NIR light irradiation to realize the transformation of hydrophobic to hydrophilic properties [26].

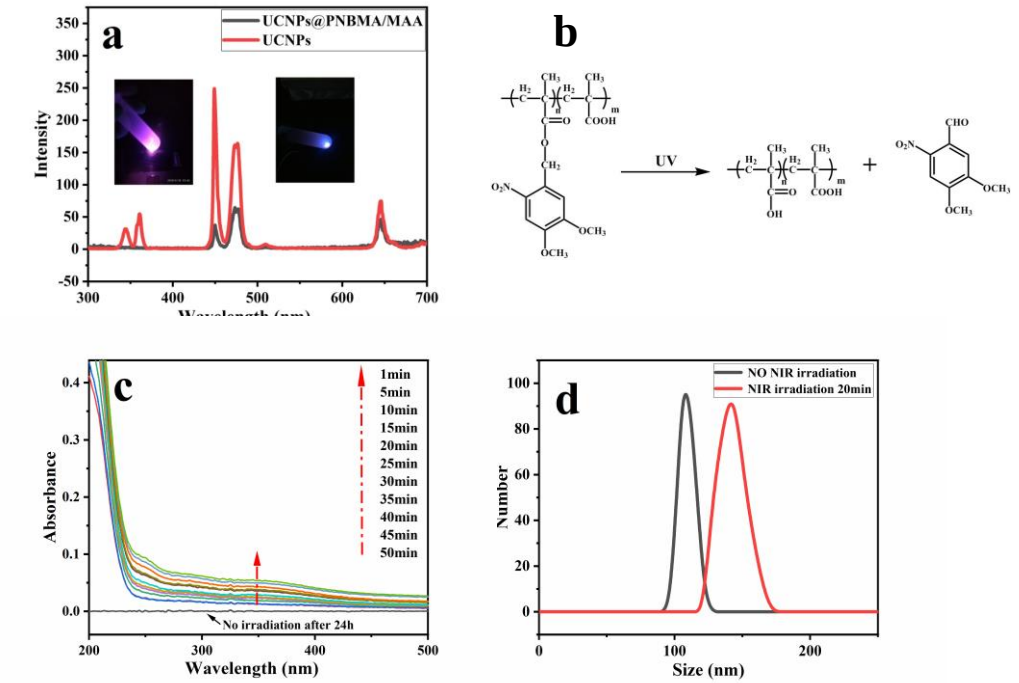

Fig. 4.(a) Upconversion luminescent spectra of UCNPs (black) and UCNPs@PNBMA/MAA (red) UCNPs and UCNPs@PNBMA/MAA nanocapsules; (b) The photo-cleavage reaction of o-nitrobenzyl ester; (c) UV spectra of UCNPs@PNBMA/MMA nanocapsules after Near infrared light irradiation; (d) Change of the size of UCNPs@PNBMA/MMA after NIR light irradiation.

3.3. Controlled release behavior of DOX-UCNPs@ PNBMA/MMA nanocapsules

UCNPs@PNBMA/MMA nanocapsules exhibit both pH and light responsive behaviors, which could be used as smart drug delivery system. Hydrochloride DOX is a hydrophilic anticancer drug, used as a model drug to investigate the loading and releasing behavior of the synthesized UCNPs@PNBMA/MAA nanocapsules. Fig. 5a shows the absorbance-concentration curve of DOX, from which the relationship between absorbance and concentration can be fitted by an equation y = 16.3x + 0.044 (R^2 = 0.99842). Fig. 5b shows the UV spectrum of the solution diluted by 10 times before and after DOX loading. The calculated DOX drug loading rate is 7.23wt%, which is competitive with the amphiphilic polymer/UCNP self-assembled system (7wt%) [33, 34] and higher than that of porous silica coating system (5wt%) [35]. However, the robust structure of the UCNPs@PNBMA/MAA nanocapsules constructed of distillation precipitation polymerization was favorable in the complex vivo system.

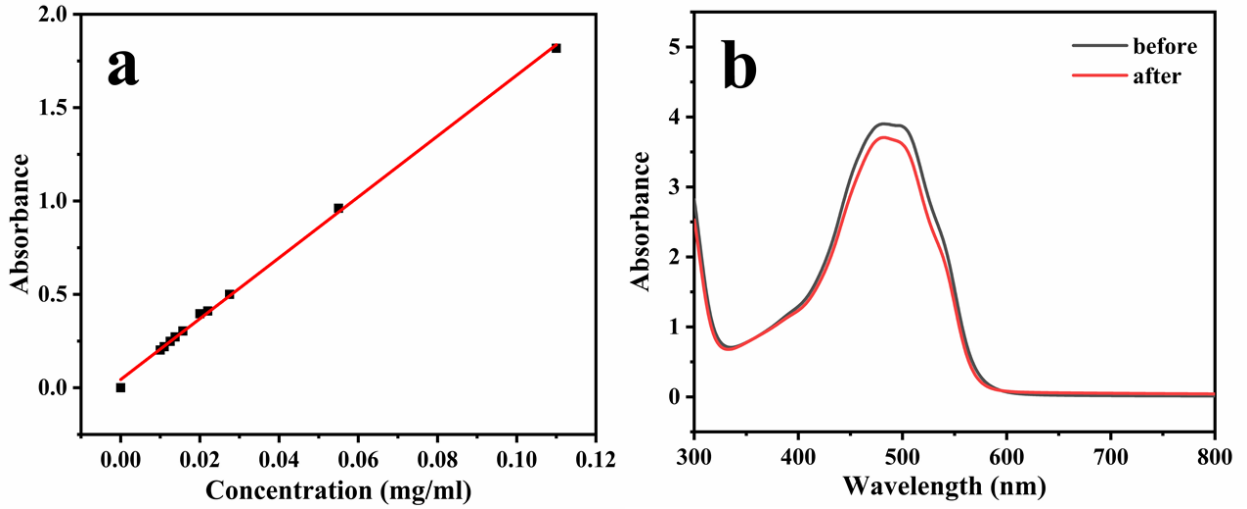

Fig. 5. (a) Absorbance-Concentration relationship of DOX. (b) UV-Vis spectra of DOX before and after drug loading (dilute 10 times).

As the UCNPs@PNBMA/MAA nanocapsules are dual-responsive, the release of drug-loaded nanocapsules, under different conditions, is investigated. Fig. 6 show the UV-Vis spectra of

DOX released from DOX-UCNPs@PNBMA/MAA nanocapsules under the condition of pH 7.4, pH 4.5, NIR and pH 4.5, respectively. At pH 7.4, the release rate of DOX is relatively slow. After 300 min, the cumulative release of DOX is only 8.35%. However, as shown in Fig. 7a, at pH 4.5, the cumulative release of DOX reached 35% in 720 min. It was mainly caused by hydrogen bond and charge action [36]. The -COOH group in PMAA (pKa 4.8) would undergo deionization or ionization in different pH environments. At pH 7.4, the ionization of carboxylic acid groups would cause the surface of the polymer to be negatively charged, which is not favorable for the release of positively charged DOX. In addition, the carboxylic acid groups would form two hydrogen bonds with the hydroxyl and amino groups in DOX molecules as shown in Scheme 2. At low pH (pH 4.5), the ionization of carboxylic acid groups weakens the charge adsorption, and the protonation of amino groups in DOX molecules could not form hydrogen bonds with carboxylic acid groups. Eventually, the release rate of DOX increased significantly.

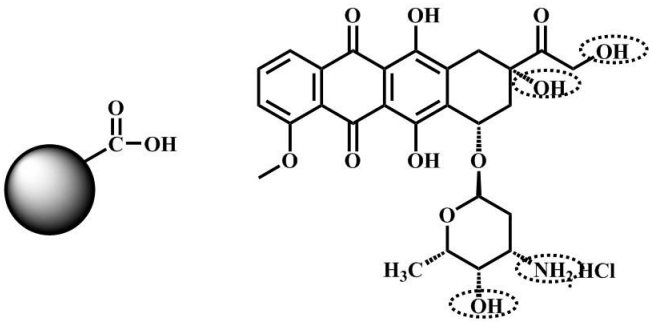

Scheme 2. Surface structure of UCNPs@PNBMA/MAA nanocapsules and chemical structure of DOX molecule.

Under NIR irradiation, the photolysis reaction of the o-nitrobenzyl would change the surface of the UCNPs@PNBMA/MAA nanocapsules from hydrophobic to hydrophilic. Furthermore, the cumulative release amount achieved 18% in 240 min. When NIR light irradiation and pH

stimulation were both carried on, the release rate and amount of DOX would further increase. As shown in Fig. 6d, the cumulative release amount of DOX reached 59.5% in 300 min. The synergistic effect from different stimulus is in favor of the release rate in many works [37-39]. It not only realizes the double responsive release, but also greatly increases the release efficiency.

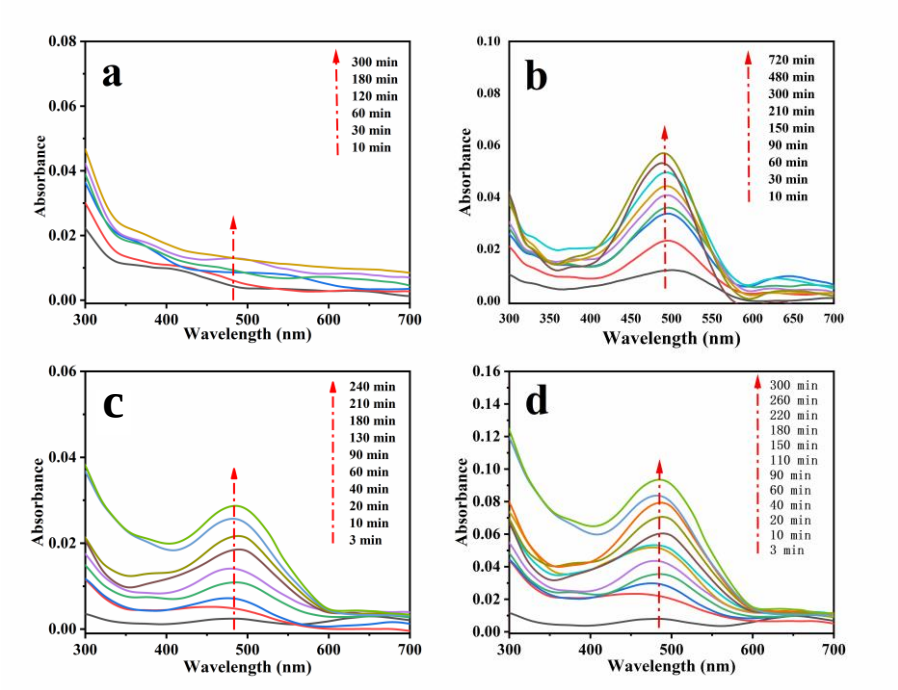

Fig. 6. The absorbance change of released DOX of DOX-UCNPs@PNBMA/MAA of DOX from UCNPs@PNBMA/MAA as a function of time under (a) pH 7.4, (b) pH 4.5, (c) NIR and (d) NIR and pH 4.5.

Due to the difference of the matrices, there are also multiple models for the drug release process [40-43]. Among them, the Baker-Lonsdale model is more suitable for spherical matrices and modeling the drug release behavior under different conditions in this work. The expression is as Equ. 1. Fig. 7 indicated the cumulative release of DOX from UCNPs@PNBMA/MAA under different conditions, pH 7.4, pH 4.5, NIR and NIR/pH 4.5 and linear regression analysis using

the Baker−Lonsdale model profile of DOX from UCNPs@PNBMA/MAA nanocapsules as a function of time under different conditions.

$$\frac{3}{2}\left[1-\left(1-\frac{M_t}{M_\infty}\right)^{\frac{2}{3}}\right]-\frac{M_t}{M_\infty}=\frac{3DC_s}{r_0^2C_0}\cdot t \quad (1)$$

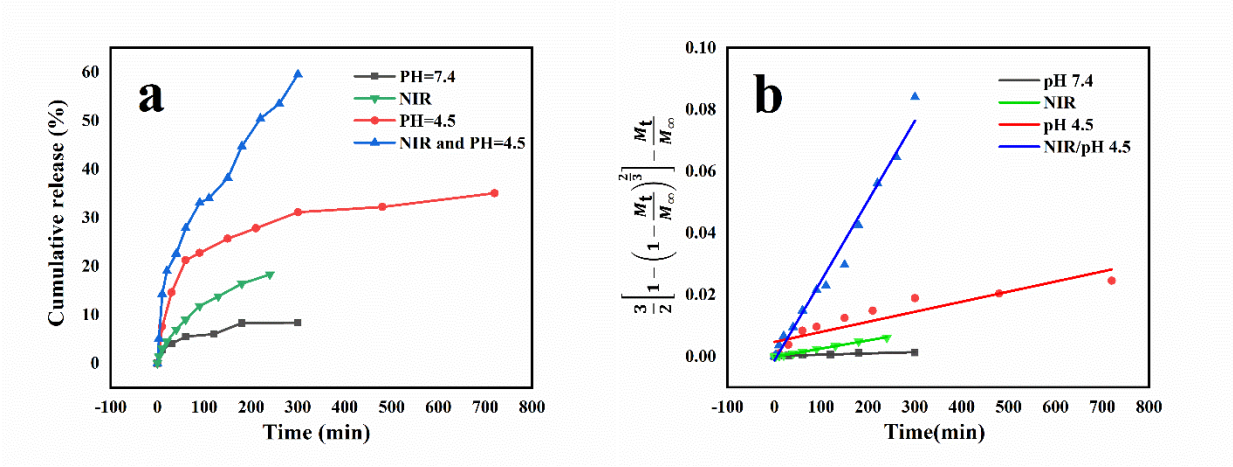

Fig. 7. (a) Cumulative release of DOX from UCNPs@PNBMA/MAA nanocapsules under different conditions: pH 7.4, pH 4.5, NIR and NIR/pH 4.5. (b) Linear regression analysis using the Baker−Lonsdale model profile of DOX from UCNPs@PNBMA/MAA nanocapsules as a function of time under different conditions.

Where M_t and M_∞ are expressed as the release amount of DOX at time t and infinity, respectively; M_t/M_∞ is expressed as the cumulative release percentage of DOX at time t; D is expressed as the diffusion coefficient of the DOX from the system; C_s is expressed as the solubility of the DOX in the system; C_0 is the original concentration of DOX, r_0 is expressed as the radius of the nanoparticles. As shown in Fig. 7b, the release rate constants ($3DC_s/r_0^2C_0$) and the correlation coefficients R^2 are 4.15×10^{-6} and 0.98 (pH 7.4 and visible light), $2.64 \times 10^{-5}$and 0.99 (NIR light), 3.26×10^{-5} and 0.97 (pH 4.5 and visible light), 2.59×10^{-4} and 0.99 (pH 4.5 and NIR light), respectively. The results indicate that the Baker-Lonsdale model well fits for the

release profile of DOX under different pH values and NIR irradiation conditions. Because in the same system, C_0 and C_s are generally considered as equal, and the value of r_0 is determined from Fig.7. It can be seen that the diffusion coefficient D under the pH 4.5 is 4.1 times higher than the pH 7.4. Under the condition of pH 4.5, the diffusion coefficient D_r under NIR irradiation is 13 times higher than the visible light irradiation. The result proves that both NIR and acidic conditions are beneficial for drug release. In fact, the pH value of normal tissues and organs in human body is about 7.4, while the pH value in tumor tissue is acidic. There are a few composite systems constructed of poly-o-nitrobenzyl and UCNP self-assembled system which could achieve controlled release upon NIR irradiation due to the disassemble of the composite. Our work developed drug loaded UCNPs/PNBMA nanocarriers with stable structures and NIR/pH dual adjustable release rate which has great potential on improving drug efficacy and preventing undesirable side effects on normal tissue.

4. Conclusions

In this study, the distillation precipitation method was used to synthesize dual-responsive drug delivery nanocapsules, which was composed of a UCNP core and a transformable poly-o-nitrobenzyl shell. Hydrophobic-hydrophilic transformation could be realized upon NIR irradiation, leading to the cleavage of poly-o-nitrobenzyl ester side group and larger particle size from 108 nm to 140 nm. Hydrogen bond and charge action of DOX and nanocapsules caused the pH responsive release behavior. DOX could be loaded into these nanocomposites with a loading efficiency of 7.23 wt%. Under the synergistic effect of pH 4.5 and NIR irradiation, the cumulative release rate can reach 59.5% after 300 min. Finally, diffusion coefficient ($3DC_s/r_0^2C_0$) and R^2 under different conditions were determined to be 4.15×10^{-6} and 0.98 (pH 7.4 and visible light), $2.64 \times 10^{-5}$and 0.99 (NIR light), 3.26×10^{-5} and 0.97 (pH 4.5 and visible light), 2.59×10^{-4}

and 0.99 (pH 4.5 and NIR light) according to Baker-Lonsdale model, respectively. It shows that both NIR irradiation and acidic conditions are beneficial to drug release. This controlled release feature makes the nanocomposite a promising therapeutic agent for treating diseases.

Acknowledgements

This work was supported by the National Natural Science Foundation of China (51303049, 31871442 and 51973072).

Supporting Information Available

Supporting Information includes: Fourier transform infrared spectra of OA–UCNPs, UCNPs@SiO_2 and UCNPs@SiO_2@PNBMA/MMA. TEM images of particles prepared under different crosslink in gagent. Changes in ion energy level and luminescence principle.

References

[1] L.J. Shi, Y. Jin, W.N. Du, S.Q. Lai, Y.C. Shen, R. Zhou, Diselenide-containing nonionic gemini polymeric micelles as a smart redox-responsive carrier for potential programmable drug release, Polymer 198 (2020) 122551.

[2] N.S. Satarkar, D. Biswal, J.Z. Hilt. Hydrogel nanocomposites: A review of applications as remote controlled biomaterials, Soft Matter 6 (2010) 2364−2371.

[3] N. Suchao-in, S. Chirachanchai, S. Perrier, pH- and thermo-multi-responsive fluorescent micelles from block copolymers viareversible addition fragmentation chain transfer (RAFT) polymerization, Polymer 50 (2009) 4151−4158.

[4] Z. Feng, L. Lin, Z. Yan, Y. Yu, Dual responsive block copolymer micelles functionalized by NIPAM and azobenzene, Macromol. Rapid. Commun. 31 (2010) 640−644.

[5] S. Sutthasupa, K. Faungnawakij, K.B. Wagener, F. Sanda, Thermo-responsive micelles prepared from brush-like block copolymers of proline- and oligo (lactide)-functionalized norbornenes, Polymer 177 (2019) 178−188.

[6] Q. Yan, L. Liu, T. Wang, H. Wang, A pH-responsive hydrogel system based on cellulose and dopamine with controlled hydrophobic drug delivery ability and long-term bacteriostatic property, Colloid Polym. Sci. 297 (2019) 705−717.

[7] K.B. Sutradhar, C.D. Sumi, Implantable microchip: The futuristic controlled drug delivery system, Drug Deliv. 23 (2016) 1−11.

[8] X. Gao, Z. Yu, B. Liu, J. Yang, X. Yang, Y. Yu, A smart drug delivery system responsive to pH/enzyme stimuli based on hydrophobic modified sodium alginate, Eur. Polym. J. 133 (2020) 109779.

[9] B. Shi, X. Du, J. Chen, L. Fu, M. Morsch, A. Lee, Y. Liu, N. Cole, R. Chung, Multifunctional hybrid nanoparticles for traceable drug delivery and intracellular microenvironment-controlled multistage drug-release in neurons, Small 13 (2017) 1603966.

[10] S. Chen, Y. Gao, Z. Cao, B. Wu, L. Wang, H. Wang, Z. Dang, G. Wang, Nanocomposites of spiropyran-functionalized polymers and upconversion nanoparticles for controlled release stimulated by near-infrared light and pH, Macromolecules 49 (2016) 7490−7496.

[11] V. Marturano, H. Marcille, P. Cerruti, N.A.G. Bandeira, M. Giamberini, A. Trojanowska, B. Tylkowski, C. Carfagna, G. Ausanio, V. Ambrogi, Visible-light responsive nanocapsules for wavelength-selective release of natural active agents, ACS Appl. Nano Mater. 2 (2019) 4499−4506.

[12] K.L. Chen, S.X. Zhou, S. Yang, L.M. Wu, Fabrication of all-water-based self-repairing super hydrophobic coatings based on UV-responsive microcapsules, Adv. Funct. Mater. 25 (2015) 1035−1041.

[13] E. Blasco, J.L. Serrano, M. Piñol, L. Oriol, Light responsive vesicles based on linear dendritic block copolymers using azobenzene-aliphatic codendrons, Macromolecules 46 (2013) 5951−5960.

[14] Y. Xue, J. Tian, W. Tian, P. Gong, J. Dai, X. Wang, Significant fluorescence enhancement of spiropyran in colloidal dispersion and its light-induced size tunability for release control, J. Phys. Chem. C. 119 (2015) 20762−20772.

[15] F. Wang, H. Liu, Dual-functional emulsifying/antifogging coumarin-containing polymeric micelle, J. Phys. Chem. C. 122 (2018) 3434−3442.

[16] G. Pariani, M. Quintavalla, L. Colella, L. Oggioni, R. Castagna, F. Ortica, C. Bertarelli, A. Bianco, A new insight into the fatigue resistance of photochromic 1,2-diarylethenes, J. Phys. Chem. C. 121 (2017) 23592−23598.

[17] J. Zhang, J.K. Whitesell, M.A. Fox, Photoreactivity of self-assembled monolayers of azobenzene or stilbene derivatives capped on colloidal gold clusters, Chem. Mater. 13 (2001) 2323−2331.

[18] H.M.D. Bandarab, S.C. Burdette, Photoisomerization in different classes of azobenzene, Chem. Soc. Rev. 41 (2012) 1809−1825.

[19] R. Klajn, Spiropyran-based dynamic materials, Chem. Soc. Rev. 43 (2014) 148−184.

[20] K. Matsuda, M. Irie, Diarylethene as a photoswitching unit, J. Photochem. Photobiol. C: Photochem. Rev. 5 (2004) 169−182.

[21] T. Kudernac, S.J. van der Molen, B.J. Wees, B.L. Feringa, Uni- and bi-directional light-induced switching of diarylethenes on gold nanoparticles, Chem. Commun. 34 (2006) 3597−3599.

[22] P.U. Bastian, L. Yu, A.L. deGuereñu, R. Haag, M.U. Kumke, Bioinspired confinement of upconversion nanoparticles for improved performance in aqueous solution, J. Phys. Chem. C. 124 (2020) 28623−28635.

[23] X. Liu, R. Deng, Y. Zhang, Y. Wang, H. Chang, L. Huang, X. Liu, Probing the nature of upconversion nanocrystals: Instrumentation matters, Chem. Soc. Rev. 44 (2015) 1479−1508.

[24] J. Zhou, Q. Liu, W. Feng, Y. Sun, F. Li, Upconversion luminescent materials: Advances and applications, Chem. Rev. 115 (2015) 395−465.

[25] N.M. Idris, M.K.G. Jayakumar, A. Bansal, Y. Zhang, Upconversion nanoparticles as versatile light nanotransducers for photoactivation applications, Chem. Soc. Rev. 44 (2015) 1449−1478.

[26] B. Yan, J.C. Boyer, N.R. Branda, Y. Zhao, Near-infrared light-triggered dissociation of block copolymer micelles using upconverting nanoparticles, J. Am. Chem. Soc. 133 (2011) 19714−19717.

[27] J. Xiang, F. Ge, B. Yu, Q. Yan, F. Shi, Y. Zhao, Nanocomplexes of photolabile polyelectrolyte and upconversion nanoparticles for near-infrared light-triggered payload release, ACS Appl. Mater. Interfaces 10 (2018) 20790−20800.

[28] M.L. Viger, M. Grossman, N. Fomina, A. Almutairi, Low power upconverted near-IR light for efficient polymeric nanoparticle degradation and cargo release, Adv. Mater. 25 (2013) 3733−3738.

[29] X.T. Wang, X.P. Liu, L. Wang, C.Y. Tang, W.C. Law, G. Zhang, Y.G. Liao, C. Liu, Z.F. Liu, Synthesis of yolk-shell polymeric nanocapsules encapsulated with mono dispersed upconversion nanoparticle for dual-responsive controlled drug release, Macromolecules 51 (2018) 10074−10082.

[30] R. Weissleder, A clearer vision for in vivo imaging, Nat. Biotechnol. 19 (2001) 316−317.

[31] X.T. Wang, C. Liu, Z.H. Li, C.Y. Tang, W.C. Law, X.H. Gong, Z.F. Liu, Y.G. Liao, G.W. Zhang, S.J. Long, L. Chen, Thermal and photo dual-responsive core-shell polymeric nanocarriers with encapsulation of upconversion nanoparticles for controlled anticancer drug release, J. Phys. Chem. C. 123 (2019) 10658−10665.

[32] R.A. Jalil, Y. Zhang, Biocompatibility of silica coated $NaYF_4$ upconversion fluorescent nanocrystals, Biomaterials 29 (2008) 4122−4128.

[33] C. Wang, L. Cheng, Z. Liu, Drug delivery with upconversion nanoparticles for multi-functional targeted cancer cell imaging and therapy, Biomaterials 32 (2011) 1110−1120.

[34] G. Tian, Z. Gu, L. Zhou, W. Yin, X. Liu, L. Yan, S. Jin, W. Ren, G. Xing, S. Li, Y. Zhao, Mn^{2+} dopant-controlled synthesis of $NaYF_4$:Yb/Er upconversion nanoparticles for in vivo imaging and drug delivery, Adv. Mater. 24 (2012) 1226−1231.

[35] J. Liu, W. Bu, L. Pan, J. Shi, NIR-triggered anticancer drug delivery by upconverting nanoparticles with integrated azobenzene-modified mesoporous silica, Angew. Chem. Int. Ed. 52 (2013) 4375−4379.

[36] R. Cheng, F. Meng, C. Deng, H.A. Klok, Z. Zhong, Dual and multi-stimuli responsive polymeric nanoparticles for programmed site-specific drug delivery, Biomaterials 34 (2013) 3647−3657.

[37] X.T. Wang, T. Huang, W.C. Law, C.H. Cheng, C.Y. Tang, L. Chen, X.H. Gong, Z.F. Liu, S.J. Long, Controlled encapsulation and release of substances based on temperature and photoresponsive nanocapsules, J. Phys. Chem. C. 122 (2018) 3039−3046.

[38] X.T. Wang, Z.H. Li, Y.K. Yang, X.H. Gong, Y.G. Liao, X.L. Xie, Photomechanically controlled encapsulation and release from pH-responsive and photoresponsive microcapsules, Langmuir 31 (2015) 5456−5463.

[39] X.T. Wang, X.P. Liu, H.D. Zhu, G.W. Zhang, X.F. Li, C.Y. Tang, W.C. Law, X. Zhao, Near infrared to ultraviolet upconversion nanocomposite for controlling the permittivity of polyspiropyran shell, Polym. Test. 94 (2021) 107042.

[40] R.W. Baker, H.K. Lonsdale, Controlled release: Mechanisms and rates. In controlled release of biologically active agents; A.C. Tanquary, R.E. Lacey, Eds., Plenum Press: New York, (1974) 15−71.

[41] H. Hu, H. Wang, Q. Du, Preparation of pH-sensitive polyacrylic acid hollow microspheres and their release properties, Soft Matter 8 (2012) 6816−6822.

[42] J.O. Kim, A.V. Kabanov, T.K. Bronich, Polymer micelles with cross-linked polyanion core for delivery of a cationic drug doxorubicin, J. Control. Release. 138 (2009) 197−204.

[43] S. Radin, T. Chen, P. Ducheyne, The controlled release of drugs from emulsified, sol gel processed silica microspheres, Biomaterials 30 (2009) 850−858.